Measurement of anomalously strong emission from the 1s-9p transition in the spectrum of H-like phosphorus following charge exchange with molecular hydrogen

M. A. Leutenegger,[1,2] P. Beiersdorfer,[3,4] G. V. Brown,[3] R. L. Kelley,[1] C. A. Kilbourne,[1] and F. S. Porter[1]

[1]*NASA Goddard Space Flight Center, Greenbelt, MD 20771*
[2]*NASA Postdoctoral Fellow*
[3]*Lawrence Livermore National Laboratory, Livermore, CA 94550*
[4]*Space Sciences Laboratory, University of California, Berkeley, CA 96720*

(Dated: July 13, 2010)

We have measured K-shell x-ray spectra of highly ionized argon and phosphorus following charge exchange with molecular hydrogen at low collision energy in an electron beam ion trap using an x-ray calorimeter array with ~6 eV resolution. We find that the emission at the high-end of the Lyman series is greater by a factor of two for phosphorus than for argon, even though the measurement was performed concurrently and the atomic numbers are similar. This does not agree with current theoretical models and deviates from the trend observed in previous measurements.

Charge exchange (CX) between neutral species and ions is important in setting the ionization balance in laboratory and astrophysical plasmas, as well as the storage time in ion traps and storage rings, anti-hydrogen production, and diagnosing fusion plasmas [1–8]. X-rays from CX between solar wind ions and neutrals in comets and planetary atmospheres are highly diagnostic of both the solar wind and the neutral species [9–12]. CX between the solar wind and neutral heliospheric gas contributes a variable background that needs to be understood in order to interpret observations of interstellar and intergalactic plasmas [13]. Solar-system CX typically occurs at low collision velocities (< 700 km/s), a previously neglected regime that has been the subject of renewed interest over the last decade [14–16].

Qualitatively, one expects CX between given neutral and highly ionized species to be dominated by capture of single electrons into states with a particular principal quantum number around $n_c \approx q^{3/4}$, where q is the charge of the capturing ion [17]. Following capture, the electron decays radiatively to the ground state, either directly or via a cascade. For bare ions, captures into $n_c p$ usually decay directly to the $1s$ ground level, while captures into higher angular momentum states will cascade on the Yrast chain ($l = n - 1$) in steps of $\Delta l, \Delta n = -1$, ultimately resulting in a $2p \rightarrow 1s$ Lyα photon.

In the limit of high collision velocity, the angular momentum distribution of captured electrons is expected to be statistical, and high angular momentum states dominate; however, at low collision velocity, high angular momentum states are not accessible [18, 19]. Because captures into $n_c p$ usually result in $n_c p \rightarrow 1s$ photons, while captures into other states usually result in Lyα photons, the ratio of flux in the $n_c p \rightarrow 1s$ transition to that in Lyα is a diagnostic of the distribution of angular momentum states populated, and thus of the collision velocity. X-ray detectors with moderate spectral resolution do not resolve the high-n Lyman series; thus it is often simpler to measure the hardness ratio, defined as $\mathcal{H} \equiv F_{3+}/F_2$, where F_2 is the observed flux of transitions from principal quantum number $n = 2$ to the ground state, and F_{3+} is the sum of flux in transitions from $n \geq 3$ to the ground state.

Beiersdorfer *et al.* [20] measured K-shell x-ray spectra from CX at low ion temperature for a wide range of ions in the Lawrence Livermore National Laboratory (LLNL) EBIT-I electron beam ion trap (EBIT) using a high purity germanium detector, with the goal of studying the angular momentum distribution of captured electrons in CX at low collision velocity. Not only was the expected deviation from a statistical population of angular momentum states found, but the observed hardness ratios were much higher than predicted in classical trajectory Monte Carlo (CTMC) theory, with a hardness ratio of about unity observed over a wide range in atomic number (10-54) for H-like species.

A subsequent experiment by the Berlin EBIT group has reproduced the measurement of the LLNL EBIT group for argon; however, when they instead extracted a beam from their EBIT and collided it with a stationary neutral argon gas target, they found significantly lower hardness ratios at collision energies comparable to those in their EBIT [21]. The lower hardness ratios in the beam experiment are consistent with the predictions of CTMC theory. Allen *et al.* [21] consider numerous factors that could affect CX either in the beam or in the trap and thus reconcile the discrepancy, including the electric and magnetic fields in the trap, the temperature of the ions in the trap, loss of photons from metastable states in the extraction experiment, and possible polarized and anisotropic emission in the extraction experiment, while emission in the trap is unpolarized and isotropic. All of these factors are considered unlikely by Allen *et al.*, with the exception of the possibility of polarization and anisotropy, which is not yet well understood in the extraction experiment.

In this paper we present high resolution x-ray spectra following CX between highly ionized argon and phosphorus with molecular hydrogen. Molecular hydrogen was

chosen because of its relative simplicity as a collision gas. We compare the spectra and find that the hardness ratio of H-like P is unexpectedly twice as large as that of H-like Ar. The experiment was performed with bare P and Ar ions co-mixed in the trap. Both ion species thus were exposed to identical experimental conditions, e.g. the same neutral gases, magnetic and electric fields, and trapping cycle length, and had the same temperature. The fact that they produce starkly varying x-ray spectra shows that the current understanding of charge exchange is insufficient and as of yet unknown physics must be included in future x-ray production models.

Our measurements were performed using the SuperEBIT electron beam ion trap at LLNL [22, and references therein], using the magnetic trapping mode [23]. Neutral P and Ar enter the trap and are subsequently ionized by the electron beam. After the desired ionization balance has been achieved, the beam is turned off, and EBIT operates as a Penning trap with the ions confined in the radial direction by the ~ 3 T magnetic field of the superconducting Helmholtz coils.

While the ions are magnetically trapped, H_2 is continuously introduced through a ballistic gas injector at a much higher partial pressure than Ar or P, and the only significant source of x-ray emission is CX events between H_2 and the ions. After most of the ions have filled the K-shell through CX, the electric potential trapping the ions along the axial direction is turned off and the trap is dumped. The trapping cycle was divided into a beam-on ionizing phase (1.73s) and a beam-off CX phase (2.23s); we excluded the first 20 ms of the CX phase from our analysis to avoid contamination from the beam-on phase.

Trace amounts of silicon, sulfur, and chlorine were also noted to contribute indigenous ions in the trap. Only the strongest transitions of these trace species were detected, and in most cases they do not blend with any features of Ar or P. The very weak emission from He-like Cl (~ 25 counts in He α) is blended with the $n = 8 - 10$ lines of He-like P (~ 6 counts for all three lines); we estimated the contribution of the blended lines (the resonance and intercombination lines, w, x, and y) from the strength of the forbidden line, z, and accounted for the blends in our modeling of the high-n He-like P lines.

The spectra were recorded using the XRS/EBIT x-ray calorimeter instrument developed at NASA Goddard Space Flight Center [24, 25]. The XRS/EBIT is a high resolution ($\sim$ 6 eV) non-dispersive spectrometer that works by accurately measuring the temperature change in absorbing pixels operated at very low temperatures (60 mK). The XRS/EBIT has 28 pixels with a 0.1-12 keV bandpass, of which 25 were operated.

The XRS/EBIT has four permanent aluminized polyimide windows that are used for optical filtering and thermal isolation of the detector and cooling system. An additional, much thicker aluminized polyimide window was used to reduce the flux of soft x-rays (mainly due to Ar and P L-shell emission) at the detector. We looked for evidence of contamination on the filters by ice or hydrocarbons using contemporaneous data from experiments using low-Z ions such as H-like carbon and oxygen. We found no evidence for excess absorption over that expected from the windows. The upper limit to the amount of material accumulated on the windows is small enough that any contaminant present would have a negligible effect on the transmission above 2 keV.

TABLE I. Normalized H-like series line strengths and hardness ratio. Filter transmission corrected line strengths are normalized to 1000 for 1s-2p. Errors are statistical only.

	Ar	P
$1s-2p$	1000	1000
$1s-3p$	176	248
$1s-4p$	78	133
$1s-5p$	53	151
$1s-6p$	102	111
$1s-7p$	103	50
$1s-8p$	20	152
$1s-9p$	66	1224
$1s-10p$	324	—
$1s-11p$	117	—
$\mathcal{H}$	1.04 ± 0.05	2.07 ± 0.12

We present the concurrently observed CX spectra in Figure 1. There is a striking difference between the two hydrogen-like spectra, i.e. the relative intensity of the emission from capture to the levels with the highest two principal quantum numbers is three times larger for P than for Ar. We measured the number of counts in all lines by fitting them with Gaussians. We corrected the measured counts for the filter transmission and computed the relative strengths of the lines in the H-like Lyman series (Table I), as well as the He-like singlet series ($1s\,np\,^1P_1 \rightarrow 1s^2\,^1S_0$) and the He α complex (Table II). The quantum efficiency of the detectors in the 2-5 keV range is nearly unity, so we do not correct for it.

Tables I and II include measurements of the hardness ratio, $\mathcal{H} \equiv F_{3+}/F_2$. In Table II, we also define a new quantity for the He-like spectrum, $\mathcal{H}' \equiv F_{3+}/F_w$ where F_w is the observed flux in the resonance line ($1s\,2p\,^1P_1 \rightarrow 1s^2\,^1S_0$). For low-$Z$ systems such as Ar and P, where transitions from $n > 2$ to ground are dominated by emission from singlet states, this has the advantage of measuring the hardness ratio only among the singlets, and does not contain information about the triplet to singlet capture ratio. Also in Table II, we give both the ratios defined in Gabriel and Jordan [26], $\mathcal{R} \equiv F_z/(F_x+F_y)$ and $\mathcal{G} \equiv (F_z + F_y + F_x)/F_w$, as well as an alternate quantity giving the ratio of triplet to singlet captures, $\mathcal{G}' \equiv (F_z + F_y + F_x)/(F_w + F_{3+})$.

In Figure 2 we plot the hardness ratios measured in

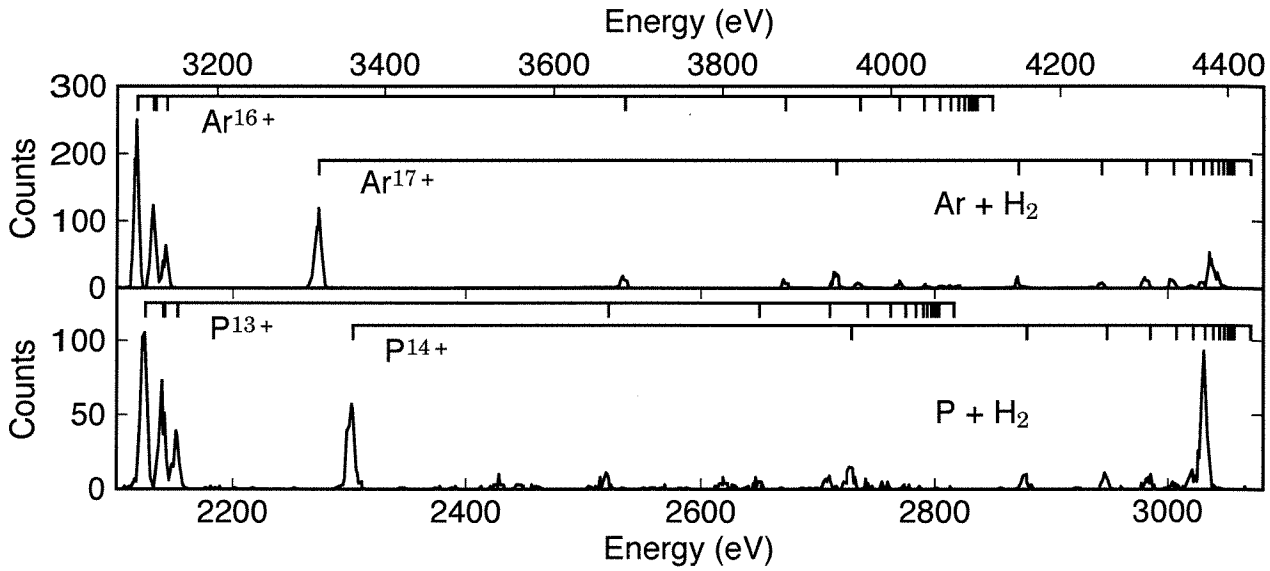

FIG. 1. X-ray emission spectra of H-like and He-like argon and phosphorus following charge exchange with molecular hydrogen. The rest energies of the series are indicated up to the $15p \rightarrow 1s$ transition, as well as the series limit.

TABLE II. Normalized He-like series line strengths and ratios. Filter transmission corrected line strengths are normalized to 1000 for w. Errors are statistical only. Definitions of the line ratios $\mathcal{R}$, $\mathcal{G}$, $\mathcal{G}'$, $\mathcal{H}$, and $\mathcal{H}'$ are given in the text.

	Ar	P
w	1000	1000
$1s-3p$	296	233
$1s-4p$	186	145
$1s-5p$	120	190
$1s-6p$	134	75
$1s-7p$	55	36
$1s-8p$	55	14
$1s-9p$	53	17
$1s-10p$	34	—
$\mathcal{R}$	1.73 ± 0.07	2.27 ± 0.15
$\mathcal{G}$	6.0 ± 0.3	4.3 ± 0.3
$\mathcal{G}'$	3.12 ± 0.13	2.55 ± 0.15
$\mathcal{H}$	0.133 ± 0.007	0.128 ± 0.010
$\mathcal{H}'$	0.93 ± 0.07	0.68 ± 0.07

Beiersdorfer *et al.* [20] and Wargelin *et al.* [27] as a function of atomic number, along with the theoretical CTMC hardness ratios computed in those papers, as well as the new measurements reported in this Letter. All of the measurements were carried out under conditions corresponding to low collision velocities. We estimate the ion temperature in the present experiment to be 450 ± 225 eV [28, 29]. For the same ion temperature, the typical collision velocity of P is slightly higher than for Ar by a factor of $\sqrt{M_{\rm Ar}/M_{\rm P}} = 1.14$.

The previous measurements are consistent with a linear, almost constant, dependence of $\mathcal{H}$ on Z (dashed line), although the CTMC predictions are lower over the whole range in Z. The hardness ratio we measure for Ar agrees very well with the earlier measurements, which indicates that we were able to reproduce the earlier experimental conditions and results. However, the new measurement of the hardness ratio of P is a factor of two greater than any of the other measurements.

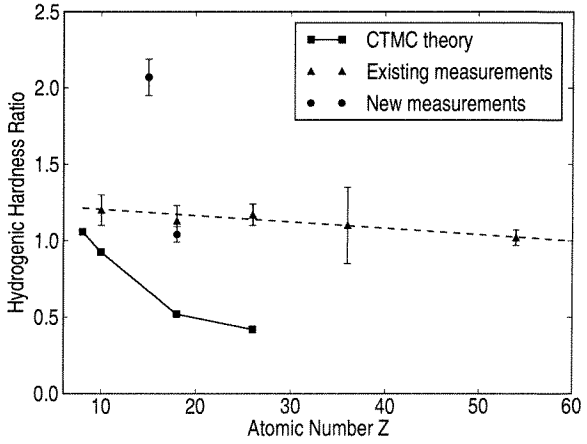

FIG. 2. Measured and calculated values of the hardness ratio of H-like CX emission as a function of atomic number Z. The dashed line gives a linear fit to the previously measured hardness ratios.

The large difference in hardness ratio we have measured for H-like P and Ar is robust, since the spectra were obtained by creating the bare ions of both elements *si-*

multaneously in the same trap, interacting with the same donor gas, and subject to the same electric and magnetic fields and trap timing cycle. Although there is some overall uncertainty in the ion temperature, and thus collision velocity, the conditions for the two ions must be comparable, since they interact with each other, are confined by the same potential, and have similar charge and mass [30].

The measured He-like spectra of Ar and P are also significantly different, as quantified by the line ratios reported in Table II. The triplet-to-singlet capture ratio $\mathcal{G}'$ for He-like Ar is consistent with three, which is expected from statistical considerations, but that of P is not. Non-statistical triplet ratios have been measured in charge exchange between N^{4+} and H or H_2 [31]. Those measurements are in agreement with the fully quantal close-coupled molecular orbital calculations of Stancil *et al.* [32]. However, in the case of our measurement it is significant that captures involving two closely neighboring ion species do not follow the same trend.

Dependence of angular momentum distributions of state-selective capture cross sections σ_{nl} on collision velocity has been reported for single electron capture onto He-like species in multiple experiments, with collision energies ranging down to 50 eV/amu [18, 33, 34]. These results could be qualitatively understood in terms of classical considerations: first, the energy levels of different angular momentum states determine their relative degree of resonance with the reaction window, which becomes narrower at low collision velocity; and second, the relative unimportance of capture into d and higher angular momentum states at low velocities can be attributed to the low classical angular momentum of the collisions. Our finding that the capture cross-section into the $9p$ state of H-like P is enhanced is surprising, since the energy splitting of the $9l$ states is much smaller than the size of the reaction window. For such highly charged ions, even the splitting between n levels is comparable to the width of the reaction window. It is understandable that capture into high l states should be negligible at the low collision velocities in EBIT, but there is no obvious reason for variations in the relative importance of capture into ns and np in Ar and P. It is likely that a fully quantal molecular orbital calculation of capture cross sections will be required to understand our results.

In summary, we have shown that two bare ion species under identical experimental conditions produce strikingly different x-ray spectra after charge exchange with H_2. The P spectrum is inconsistent with all previous measurements, including those involving lower-Z bare ions. Currently, there is no theory that suggests why this should be the case, which means that there is no *ab initio* way to predict even the gross features of an x-ray emission spectrum not yet measured in the laboratory.

We would like to acknowledge the aid of D. Thorn and J. Clementson in data acquisition; M. F. Gu for calibration support; and E. Magee for technical support. MAL is supported by an appointment to the NASA Postdoctoral Program at Goddard Space Flight Center, administered by Oak Ridge Associated Universities through a contract with NASA. Part of this work was performed by Lawrence Livermore National Laboratory under the auspices of the US Department of Energy under Contract DE-AC52-07NA27344. The XRS/EBIT instrument was constructed and maintained with support from NASA.

[1] R. C. Isler, Phys. Rev. Lett. **38**, 1359 (1977).
[2] R. J. Fonck et al., Phys. Rev. Lett. **49**, 737 (1982).
[3] R. J. Fonck and R. A. Hulse, Phys. Rev. Lett. **52**, 530 (1984).
[4] E. Källne et al., Phys. Rev. Lett. **52**, 2245 (1984).
[5] J. E. Rice et al., Phys. Rev. Lett. **56**, 50 (1986).
[6] T. Stöhlker et al., Phys. Rev. A **58**, 2043 (1998).
[7] L. Gruber et al., Phys. Rev. Lett. **86**, 636 (2001).
[8] G. Gabrielse et al., Phys. Rev. Lett. **98**, 113002 (2007).
[9] T. E. Cravens, Geophys. Res. Lett. **24**, 105 (1997).
[10] G. R. Gladstone et al., Nature (London) **415**, 1000 (2002).
[11] K. Dennerl et al., Astron. & Astrophys. **451**, 709 (2006).
[12] D. Bodewits et al., Astron. & Astrophys. **469**, 1183 (2007), arXiv:0704.1648.
[13] T. E. Cravens, Astrophys. J. Lett. **532**, L153 (2000).
[14] J. B. Greenwood et al., Astrophys. J. Lett. **533**, L175 (2000).
[15] R. J. Mawhorter et al., Phys. Rev. A **75**, 032704 (2007).
[16] B. J. Wargelin, P. Beiersdorfer, and G. V. Brown, Canadian Journal of Physics **86**, 151 (2008).
[17] R. E. Olson, Phys. Rev. A **24**, 1726 (1981).
[18] D. Dijkkamp et al., J. Phys. B **18**, 737 (1985).
[19] J. Burgdörfer, R. Morgenstern, and A. Niehaus, J. Phys. B **19**, L507 (1986).
[20] P. Beiersdorfer et al., Phys. Rev. Lett. **85**, 5090 (2000).
[21] F. I. Allen et al., Phys. Rev. A **78**, 032705 (2008).
[22] P. Beiersdorfer, Canadian Journal of Physics **86**, 1 (2008).
[23] P. Beiersdorfer et al., Rev. Sci. Inst. **67**, 3818 (1996).
[24] F. S. Porter et al., Rev. Sci. Inst. **75**, 3772 (2004).
[25] F. S. Porter et al., Canadian Journal of Physics **86**, 231 (2008).
[26] A. H. Gabriel and C. Jordan, MNRAS **145**, 241 (1969).
[27] B. J. Wargelin et al., Astrophys. J. **634**, 687 (2005).
[28] P. Beiersdorfer et al., Rev. Sci. Inst. **66**, 303 (1995).
[29] F. Currell and G. Fussmann, IEEE Transactions on Plasma Science **33**, 1763 (2005).
[30] B. M. Penetrante et al., Phys. Rev. A **43**, 4873 (1991).
[31] F. W. Bliek et al., Phys. Rev. A **57**, 221 (1998).
[32] P. C. Stancil et al., J. Phys. B **30**, 1013 (1997).
[33] D. Dijkkamp et al., J. Phys. B **18**, 4763 (1985).
[34] R. Hoekstra et al., Phys. Rev. A **41**, 4800 (1990).